

## Two layer 4:4 co-ordinated KI crystals grown within single walled carbon nanotubes

J. Sloan<sup>a</sup>, M.C. Novotny<sup>a</sup>, S.R. Bailey<sup>a</sup>, G. Brown<sup>a,b</sup>, C. Xu<sup>a</sup>, V.C. Williams<sup>a</sup>,  
S. Friedrichs<sup>a</sup>, E. Flahaut<sup>a</sup>, R.L. Callender<sup>a</sup>, A.P.E. York<sup>a</sup>, K.S. Coleman<sup>a</sup>,  
M.L.H. Green<sup>a,\*</sup>, R.E. Dunin-Borkowski<sup>b</sup>, J.L. Hutchison<sup>b</sup>

<sup>a</sup> Wolfson Catalysis Centre (Carbon Nanotechnology Group), Inorganic Chemistry Laboratory, University of Oxford,  
South Parks Road, Oxford OX1 3QR, UK

<sup>b</sup> Department of Materials, University of Oxford, Parks Road, Oxford OX1 3PH, UK

Received 25 May 2000; received in final form 21 August 2000

### Abstract

The formation of ‘all surface’ 4:4 co-ordinated KI crystals within 1.4 nm diameter single walled carbon nanotubes (SWNT) is reported. KI was inserted into the SWNTs by a capillary method [J. Sloan, D.M. Wright, H.G. Woo, S. Bailey, G. Brown, A.P.E. York, K.S. Coleman, J.L. Hutchison, M.L.H. Green, *J. Chem. Soc. Chem. Commun.* (1999) 699], whereby the nanotubes were combined intimately with the molten halide. The crystals grew with  $\langle 001 \rangle$  (relative to bulk KI) parallel to the tubule axes and were continuous tetragonally distorted bilayer crystals composed of alternating columns of K–I and I–K pairs when viewed along  $\langle 100 \rangle$ . © 2000 Elsevier Science B.V. All rights reserved.

### 1. Introduction

Single walled carbon nanotubes (SWNT) [2] can facilitate the direct observation of molecular scale species that form inside their capillaries. For example, individual endofullerenes have been imaged within SWNTs by high-resolution transmission electron microscopy (HRTEM) [3,4]. These studies are made possible by the extremely small size of SWNT capillaries, which have a median diameter of 1.2–1.6 nm. As a result, their internal surfaces act as confining van der Waals ‘cylinders’ with

internal diameters of 0.9–1.2 nm [5,6]. For encapsulated crystalline structures, these dimensions correspond to only a few atomic layers. Depending on the structure type and crystallographic orientation of the incorporated material, crystals may be obtained that are an integral number of atomic layers in thickness. For example, three atomic layer thick rocksalt-type KI crystals have been shown to form within ~1.6 nm diameter SWNTs [7].

In this Letter, we describe the formation and HRTEM examination of discrete two atomic layer thick crystals of potassium iodide within the confining surfaces of ~1.4 nm diameter SWNTs. These bilayer crystals are ‘all surface’ and have no internal atoms. We also describe significant lattice distortions from the bulk

\* Corresponding author. Fax: +44-1865-272-690.

E-mail address: malcolm.green@chem.ox.ac.uk (M.L.H. Green).

crystal structure within the SWNT incorporated KI crystals.

## 2. Experimental

SWNTs formed via arc synthesis [5] were filled with highly pure KI (Aldrich, 99.99%) by heating a mixture of as-made SWNTs with the molten iodide at 954 K, according to the capillary technique described previously [1]. The product was examined in a 300 kV JEOL JEM-3000F field emission gun HRTEM, which has a spherical aberration coefficient ( $C_s$ ) of 0.57 mm and a point resolution of 0.16 nm. Images were acquired digitally on a Gatan model 794 (1 k × 1 k) CCD camera, and the magnification was calibrated accurately using Si(110) lattice fringes. Measurements were obtained directly from HRTEM images and also fast Fourier transforms (FFT) obtained from selected areas of lattice images with the program Digital Micrograph (Gatan).

Image simulations were performed using a standard multi-slice algorithm incorporating representative parameters for a high-resolution image taken on the JEOL JEM-3000F, i.e. a focal spread of 8 nm, a beam semiconvergence of 0.6 mrad and an objective aperture of 0.1 nm. Nanotube coordinates for a (10,10) SWNT were generated using an algo-

rithm developed by White et al. [8]. Coordinates for the KI crystal were initially determined from the published KI crystal structure [9]. Lattice distortions were introduced into the KI bilayer crystal in order to mimic those observed experimentally.

## 3. Results and discussion

Fig. 1a,b shows unprocessed HRTEM images of bilayer KI crystals incorporated within a discrete SWNT and a tubule formed on the periphery of a bundle of SWNTs, respectively. The filled tubules in Fig. 1a,b both have diameters of ca. 1.35 nm, which is close to the diameter of a (10,10) SWNT [10]. Individual bilayer crystals formed inside the tubules could exhibit lengths up to the micrometer range and always form in a preferred orientation, with the rocksalt (001) direction parallel to the tubule axes. Successive dark spots along and across the tubules correspond to alternating two atom high columns of K–I and I–K. As each column contains the same pair of atoms in projection, all spots image with identical contrast as confirmed by image simulations (see below). In SWNTs with diameters larger than 1.35 nm, crystal thicknesses of three or more layers usually displayed similar preferred orientations to the bilayer crystals.

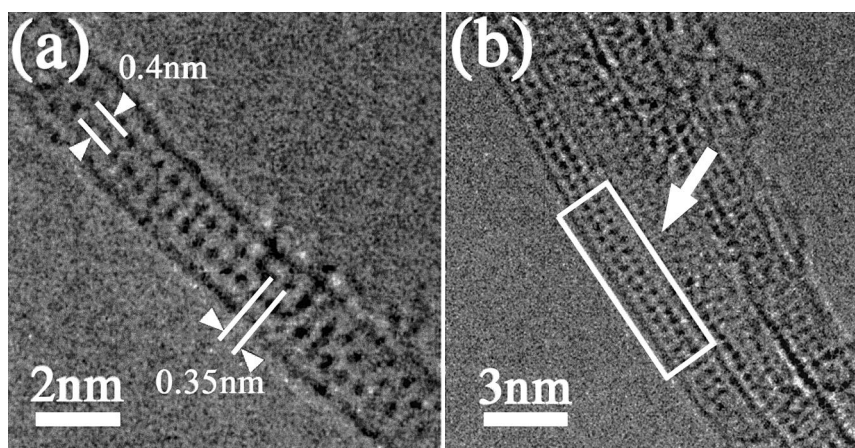


Fig. 1. (a) HRTEM image of a two atom thick KI crystal formed within a discrete 1.4 nm diameter SWNT. Each dark spot corresponds to a two atom K–I (or I–K) column. The inter-spot spacing along the tubule is ca. 0.35 nm, while across the tubule the spacing increases to 0.4 nm; (b) HRTEM image of a bundle of KI filled SWNTs. The leftmost SWNT contains a well-defined bilayer crystal.

Significant lattice distortions were observed in the bilayer crystals. Direct lattice measurements from the images showed that along the SWNT capillaries, the spots are spaced at average intervals of  $\sim 0.35$  nm, corresponding to the 0.353 nm  $\{200\}$  d-spacing of rocksalt KI [9], whereas across the SWNT capillary the spacing increases to  $\sim 0.4$  nm. The average spot spacing along the SWNTs was obtained from line profiles obtained from groups of 10–20 dark spots adjacent to the tubule walls. This produced an overall average spacing of 0.346 nm with a standard deviation (S.D.) of 0.003 nm. Measurement of the d-spacings across the SWNT capillaries had a lower degree of precision. Measurements from 40 pairs of dots produced an average spacing of 0.398 nm with a S.D. of 0.031 nm. An additional systematic error is present in both sets of measurements as a result of the magnification calibration although this will not influence the measured aspect ratio of  $\sim 1.14$ .

Further information regarding the bilayer crystals can be obtained from FFTs obtained from lattice images. In Fig. 2, **I(i)** shows a detail from Fig. 1a while **I(ii)** shows the corresponding FFT. Inspection of the latter reveals that it contains two overlapping components: a diffuse diagonal streak conforming to the SWNT and four bright spots

corresponding to the bilayer crystal. In **II(i)** and **(ii)** an image simulation and corresponding FFT of a KI/SWNT composite are shown. If the KI/SWNT composite is separated into a discrete SWNT and bilayer crystal, as shown in **I(iii)** and **II(iii)**, respectively, then the corresponding FFTs (i.e. **I(iv)** and **II(iv)**) show the components contributing to **II(ii)**. The FFT obtained from the simulated SWNT (i.e. **I(iv)**) corresponds to the Fourier transform of a projected carbon cylinder [11,12]. As the experimental HRTEM image is noisy, the fine detail of the cylinder is lost and a diffuse streak is obtained in the experimental FFT (i.e., **I(i)**) in addition to the four bright spots corresponding to the KI crystal. The latter may be used to obtain values for the lattice spacings along and across the SWNTs. Reciprocal spot spacings measured from 10 FFTs obtained from different regions of Fig. 1a,b gave average lattice spacings of 0.351 (S.D. = 0.009) along the SWNTs and 0.410 nm (S.D. = 0.019) across the SWNTs. To within experimental error, these values are consistent with the direct measurements described above.

The structural model used for the image simulations is shown in Fig. 3a,b. Fig. 3a shows a cutaway view of the bilayer crystal as viewed in

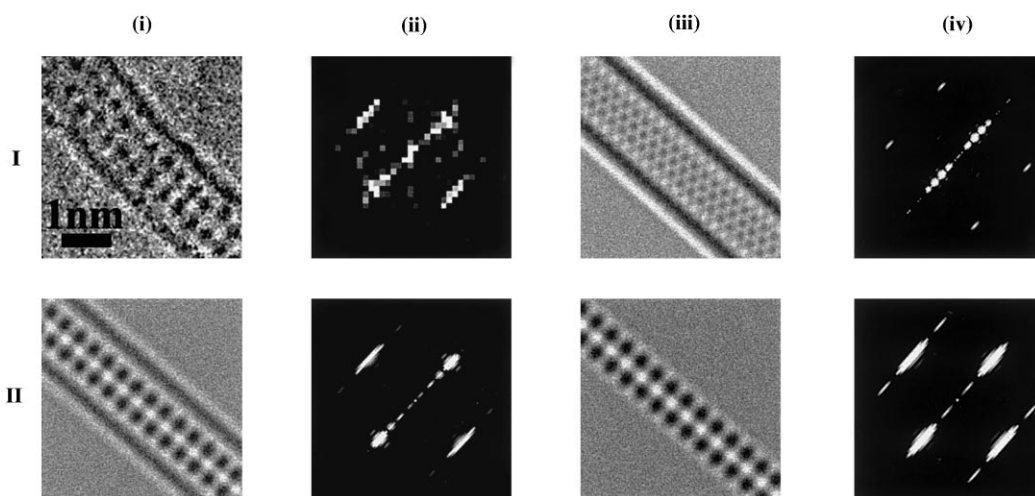


Fig. 2. **I(i)** and **II(ii)** experimental image and FFT of a bilayer KI crystal in a  $\sim 1.4$  nm diameter SWNT. **II(i)** and **II(ii)** simulated image and corresponding FFT of a KI/SWNT composite (see Fig. 3). **I(iii)** and **I(iv)** simulated image and corresponding FFT of a (10,10) SWNT. **II(iii)** and **II(iv)** simulated image and corresponding FFT of a bilayer KI crystal in a vacuum.

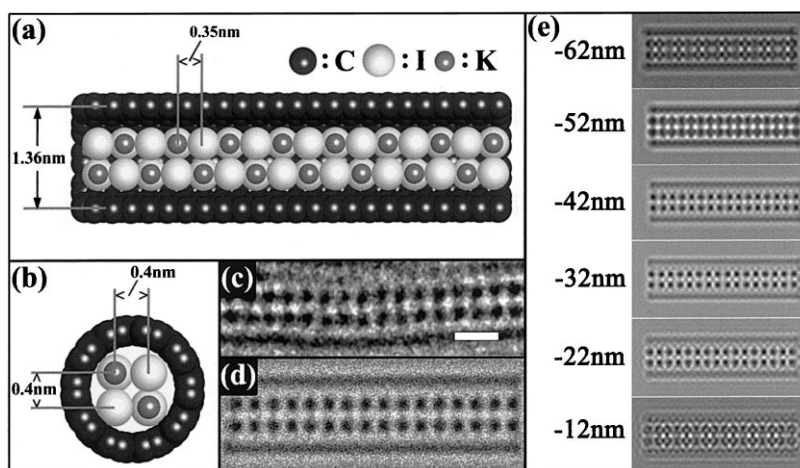


Fig. 3. (a) Cutaway structural representation of the KI/SWNT composite model used in the simulation calculations. Along the SWNT, the K–I and I–K columns are spaced at 0.35 nm. (b) End-on structural representation of (a), showing an increased lattice spacing of 0.4 nm across the capillary in two directions (assuming a symmetrical distortion). (c) Enlarged region obtained from the region arrowed in (b). (d) Image simulation computed for  $-42$  nm defocus for an undistorted bilayer KI crystal within a (10,10) SWNT. (e) Calculated through focal series of a bilayer crystal within a (10,10) SWNT.

side-on projection. Along the tube, the bulk KI spacing is maintained. Fig. 3b shows an end-on projection of the crystal with the measured lattice distortion introduced symmetrically. Fig. 3c,d show an enlargement from the arrowed region in Fig. 1b and a simulated image calculated for Scherzer defocus ( $-42$  nm for our instrument), respectively, with noise added to mimic the experimental conditions. In both images, a constant aspect ratio of  $\sim 1.14$  is maintained between the separations of dark spots measured along and across the SWNTs, respectively. In Fig. 3e, a simulated through focal series of images for the bilayer crystal is shown. The focal range over which the bilayer crystal is clearly visible is quite narrow (ca.  $-20$  to  $-50$  nm) which agrees well with similar calculations obtained for chains of  $C_{60}$  and  $C_{80}$  molecules incorporated within SWNTs [4]. In our multi-slice calculations, it was not necessary to slice the KI/SWNT composite in projection as these crystals are close to being perfect phase objects of known crystal thickness.

The observed lattice distortions could arise as consequence of two related effects – an interaction between the KI crystal and the tubule wall and a difference in K:I co-ordination from the bulk crystal. The rocksalt form of potassium iodide has

a co-ordination of 6:6 whereas, within the confines of the SWNT (see Fig. 3a,b) the net coordination is reduced to 4:4. The repeat unit of the incorporated KI crystal, in which every atom is a surface atom, is  $4/9$  of the conventional KI rocksalt unit cell (which usually has an  $a_0$  of 0.705 nm [9]) when viewed along the tubule (Fig. 2b). This reduction in coordination occurs in a highly asymmetric fashion with the four nearest neighbours of each atom in the bilayer crystal forming on only four of the six conventional octahedral sites. As a result one might expect to see differential radial displacements of the K and I positions across the tubule, as we have reported for a three layer KI crystal [7]. However no staggering of spot positions between adjacent K–I and I–K columns could be detected either in the lattice images or in simulations, probably due to the dominance of the iodine in forming the image contrast.

Hsu et al. [13] have recently reported the incorporation of KCl within the walls and capillaries of multi-walled carbon nanotubes (MWNT), formed by the reaction of  $CCl_4$  with potassium-intercalated nanotubes. As with the KI crystals described here and elsewhere [7], the MWNT intercalated KCl crystals formed with a preferred  $\langle 001 \rangle$  orientation (relative to bulk KCl) parallel to

the tubule axes, irrespective of whether the crystals were incorporated into the MWNT capillaries or into their walls. KCl crystals down to  $\sim 6$  atoms thick in cross-section were observed within the MWNT walls. Although these results provide a useful comparison with the present work, the internal diameters of MWNT tubules in which capillary crystallisation was observed were significantly larger ( $>5$  nm) than those described in this study and in Ref. [7]. For the wall intercalated KCl, it is also not possible to know the thickness of the crystals when viewed in projection.

In conclusion, this is to our knowledge the first example of an isolated and ordered two atomic layer thick crystalline material formed within a discrete porous structure. From the point of view of structural chemistry, the result is highly significant as it leads to a reduction in the coordination of the incorporated structure, a result only possible for an ‘all surface’ crystal confined in a very specific way. While such structures have been predicted theoretically [14], this is the first time that an extended bilayer crystal has been observed experimentally. The resulting KI/SWNT composite is a highly anisotropic 1D structure whose electronic and optical properties must be considerably modified with respect to both the bulk halide and the encapsulating nanotube.

### Acknowledgements

We acknowledge the Petroleum Research Fund, administered by the American Chemical Society (Grant No. 33765-AC5), the EPSRC (Grant Nos. GR/L59238 and GR/L22324) and Colebrand Ltd. for financial support. C.X. is grateful for a K.C. Wong Scholarship (University of Oxford), a Light Senior Scholarship (St Catherine’s College, Ox-

ford) and the Henry Lester trust. S.F. is indebted to BMBF and to the Fonds der Chemischen Industrie for additional financial support (Grant Nos. GR/L59238 and GR/L22324) and Colebrand Ltd. for financial support. We also thank Adam Palser and David E. Manolopolous, of The Physical and Theoretical Chemistry Laboratory, Oxford, for supplying the routine used to calculate nanotube coordinates.

### References

- [1] J. Sloan, D.M. Wright, H.G. Woo, S. Bailey, G. Brown, A.P.E. York, K.S. Coleman, J.L. Hutchison, M.L.H. Green, *J. Chem. Soc. Chem. Commun.* (1999) 699.
- [2] S. Iijima, T. Ichihashi, *Nature* 363 (1993) 603.
- [3] B.W. Smith, M. Monthieux, D.E. Luzzi, *Nature* 396 (1998) 323.
- [4] J. Sloan, R.E. Dunin-Borkowski, J.L. Hutchison, K.S. Coleman, V.C. Williams, J.B. Claridge, A.P.E. York, C. Xu, S.R. Bailey, G. Brown, S. Friedrichs, M.L.H. Green, *Chem. Phys. Lett.* 316 (2000) 191.
- [5] P. Nikolaev, A. Thess, A.G. Rinzler, D.T. Colbert, R.E. Smalley, *Chem. Phys. Lett.* 266 (1997) 422.
- [6] C. Journet, W.K. Maser, P. Bernier, A. Loiseau, M. Lamy, M.L. de la Chapelle, S. Lefrant, P. Darnier, J.E. Fisher, *Nature* 388 (1997) 756.
- [7] R.R. Meyer, J. Sloan, R.E. Dunin-Borkowski, A.I. Kirkland, M.C. Novotny, S.R. Bailey, J.L. Hutchison, M.L.H. Green, *Science* 289 (2000) 1324.
- [8] C.T. White, D.H. Robertson, J.W. Mintmire, *Phys. Rev. B* 47 (1993) 5485.
- [9] M. Ahtee, *Annal. Acad. Sci. Fenn. Ser. A* 6 (313) (1969) 1.
- [10] M.S. Dresselhaus, G. Dresselhaus, R. Saito, *Carbon* 33 (1995) 883.
- [11] Ph. Lambin, A.A. Lucas, *Phys. Rev. B* 56 (1997) 3571.
- [12] J.M. Cowley, F.A. Sundell, *Ultramicroscopy* 68 (1997) 1.
- [13] W.K. Hsu, W.Z. Li, Y.Q. Zhu, N. Grobert, M. Terrones, H. Terrones, N. Yao, J.P. Zhang, S. Firth, R.J.H. Clark, A.K. Cheetham, J.P. Hare, H.W. Kroto, D.R.M. Walton, *Chem. Phys. Lett.* 317 (2000) 77.
- [14] J. Diefenbach, T.P. Martin, *J. Chem. Phys.* 83 (1985) 4585.